Electronic Supplementary Information

A biocomputing platform with electrochemical and fluorescent signal outputs based on multi-sensitive copolymer film electrodes with entrapped Au nanoclusters and tetraphenylethene and electrocatalysis of NADH

Jiying Liang,[a] Wenting Wei,[a] Huiqin Yao,[b] Keren Shi,[c] Hongyun Liu[a] *

[a] College of Chemistry, Beijing Normal University, Beijing 100875, P. R. China

[b] School of Basic Medicine, Ningxia Medical University, Yinchuan 750004, P. R. China

[c] State Key Laboratory of High-efficiency Utilization of Coal and Green Chemical Engineering, Ningxia, Yinchuan 750021, P. R. China

*Corresponding author: Hongyun Liu, 19, Xinjiekouwai Street, Haidian District, Beijing 100875, People's Republic of China. Tel: (86)-10-58807843. E-mail: liuhongyun@bnu.edu.cn.

3.1 Characterization of AuNCs and P(DMA-*co*-NIPA)/AuNCs/TPE films

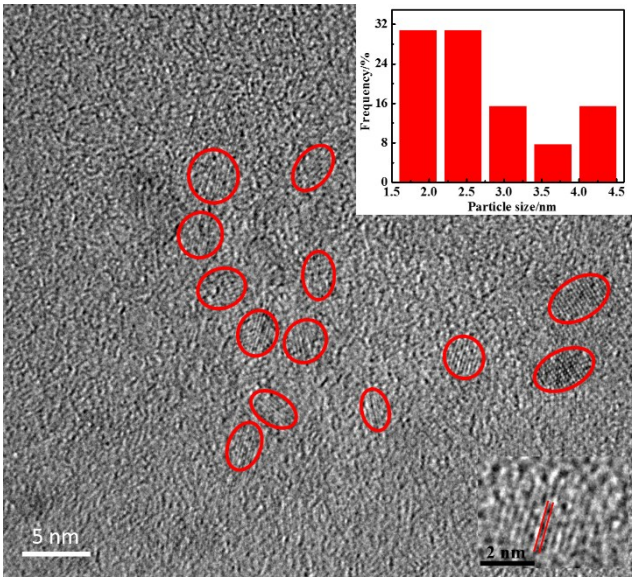

Fig. S1 HRTEM images of the Au NCs. The red circles represented the Au NCs. Inset: The frequency of different size distribution for the AuNCs in the TEM image.

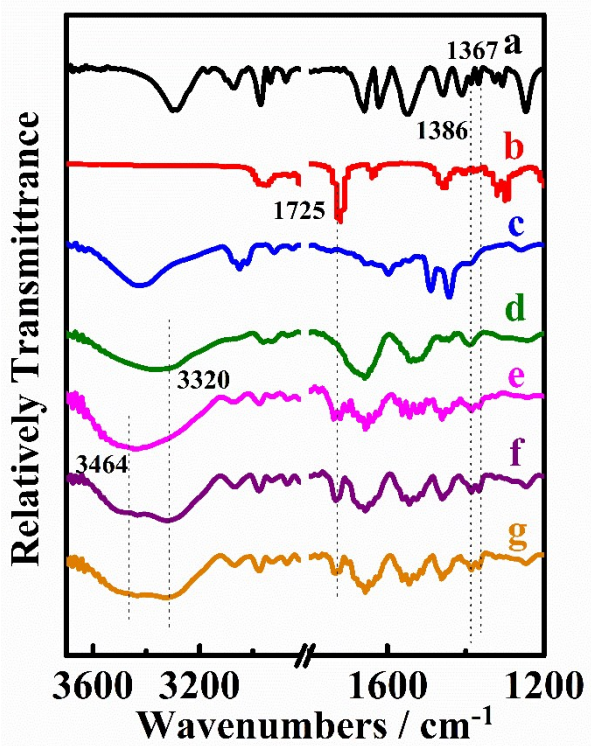

Fig. S2 IR spectra of (a) NIPA, (b) DMA, (c) TPE, (d) BSA, (e) P(DMA-*co*-NIPA), (f) P(DMA-*co*-NIPA)/AuNCs and (g) P(DMA-*co*-NIPA)/AuNCs/TPE samples.

Table S1 Assignment of characteristic IR absorption peaks for different samples

Samples	Wavenumbers (cm^{-1})			
	$\sigma_{-CH(CH_3)_2}$	ν	$\sigma_{C-O\ ester\ group}$	ν_{N-H}
NIPA	1367, 1386	-	-	-
DMA	-	-	1725	-
TPE	-	1440, 1490	-	-
BSA	-	-	-	3320
P(DMA-*co*-NIPA)	1367, 1386	-	1725	-
P(DMA-*co*-NIPA)/AuNCs	1367, 1386	-	1725	3320
P(DMA-*co*-NIPA)/AuNCs/TPE	1367, 1386	hard to distinguish	1725	3320

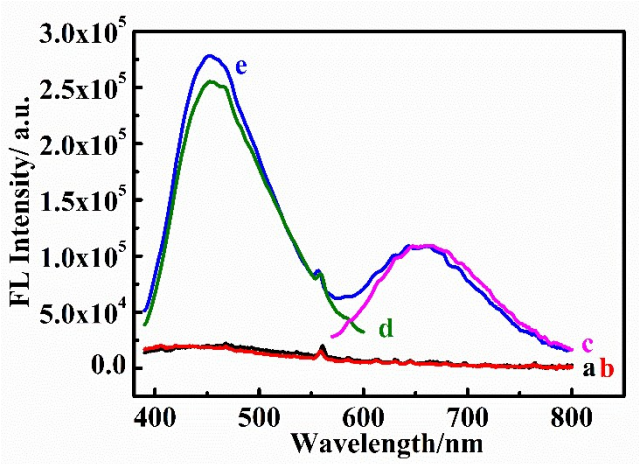

Fig. S3 Fluorescence emission spectra of (a) bare Au electrodes, (b) P(DMA-*co*-NIPA), (c) P(DMA-*co*-NIPA)/AuNCs, (d) P(DMA-*co*-NIPA)/TPE and (e) P(DMA-*co*-NIPA)/AuNCs/TPE film electrodes in pH 5.0 buffers under the excitation at 330 nm.

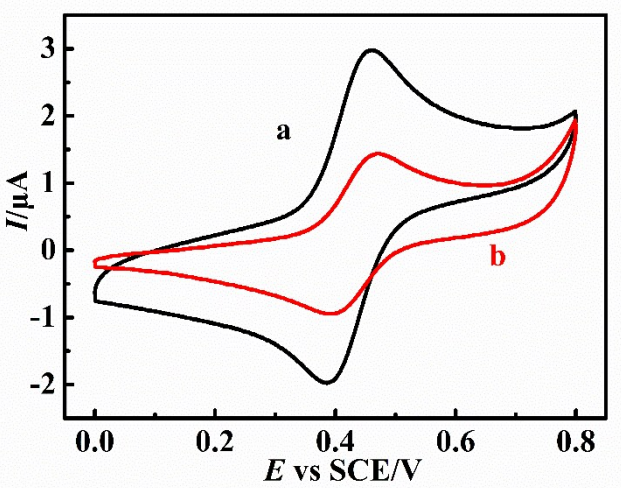

Fig. S4 CVs of 0.5 mM FDA at 0.1 V s^{-1} in pH 5.0 buffers at (a) bare Au electrodes and (b) P(DMA-*co*-NIPA)/AuNCs/TPE film electrodes.

Table S2 Estimated apparent diffusion coefficients (D') of FDA at different electrodes in pH 5.0 and 9.0 buffers

Film electrodes	$D' \times 10^6/cm^2s^{-1}$	
	pH 5.0	pH 9.0
Bare Au	7.46	7.46
P(DMA-*co*-NIPA)/AuNCs/TPE	2.04	0.21
PDMA	7.00	2.14
PNIPA	0.14	0.11
P(DMA-*co*-NIPA)	2.00	0.22
P(DMA-*co*-NIPA)/AuNCs	1.57	0.05
P(DMA-*co*-NIPA)/TPE	2.25	0.04

3.2 pH-sensitive CV property of FDA at P(DMA-*co*-NIPA)/AuNCs/TPE film electrodes

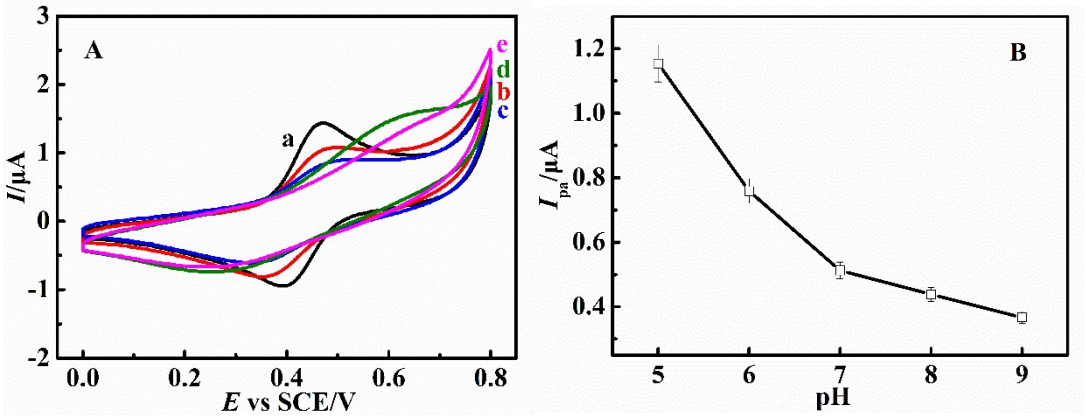

Fig. S5 (A) CVs of 0.5 mM FDA at 0.1 V s^{-1} for P(DMA-*co*-NIPA)/AuNCs/TPE films in buffers at different pH: (a) 5.0, (b) 6.0, (c) 7.0, (d) 8.0, and (e) 9.0. (B) Influence of pH on CV I_{pa} of FDA at P(DMA-*co*-NIPA)/AuNCs/TPE film electrodes.

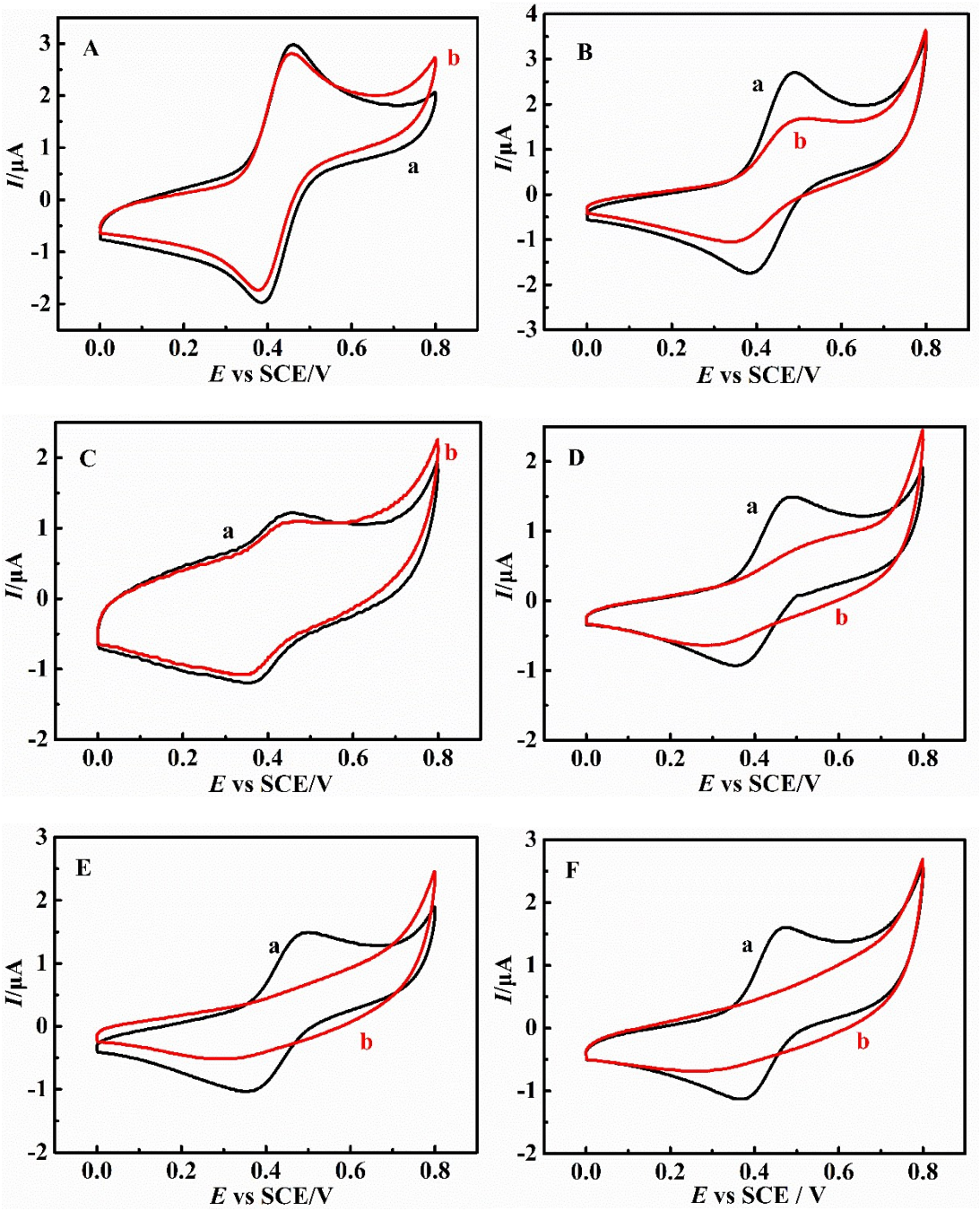

Fig. S6 CVs of 0.5 mM FDA at 0.1 V s^{-1} at (A) bare Au, (B) PDMA, (C) PNIPA, (D) P(DMA-*co*-NIPA), (E) P(DMA-*co*-NIPA)/AuNCs and (F) P(DMA-*co*-NIPA)/TPE film electrodes in buffers at pH (a) 5.0 and (b) 9.0, respectively.

3.3 SO_4^{2-}-responsive CV behavior of FDA at P(DMA-*co*-NIPA)/AuNCs/TPE film electrodes

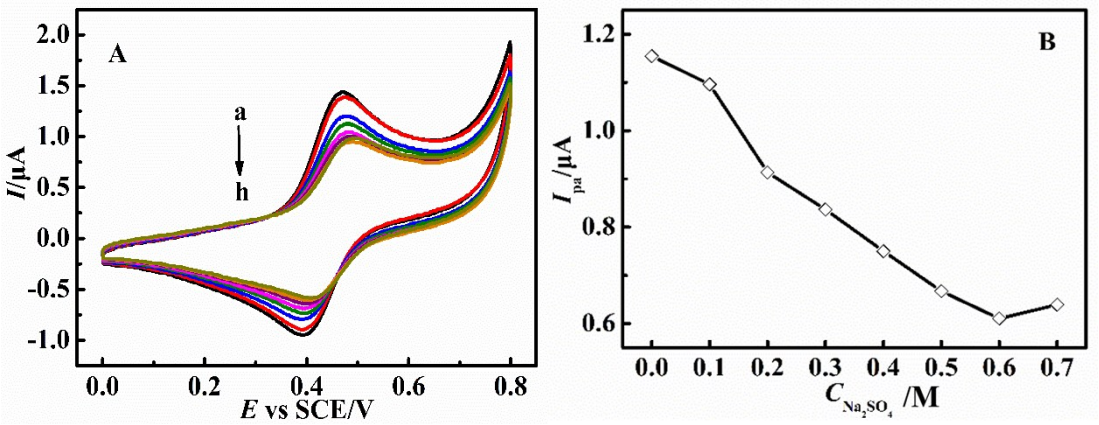

Fig. S7 (A) CVs of 0.5 mM FDA at 0.1 V s^{-1} for P(DMA-*co*-NIPA)/AuNCs/TPE films in pH 5.0 buffers containing (a) 0, (b) 0.1, (c) 0.2, (d) 0.3, (e) 0.4, (f) 0.5, (g) 0.6 and (h) 0.7 M Na_2SO_4. (B) Influence of Na_2SO_4 concentration ($C_{Na_2SO_4}$) on CV I_{pa} of FDA.

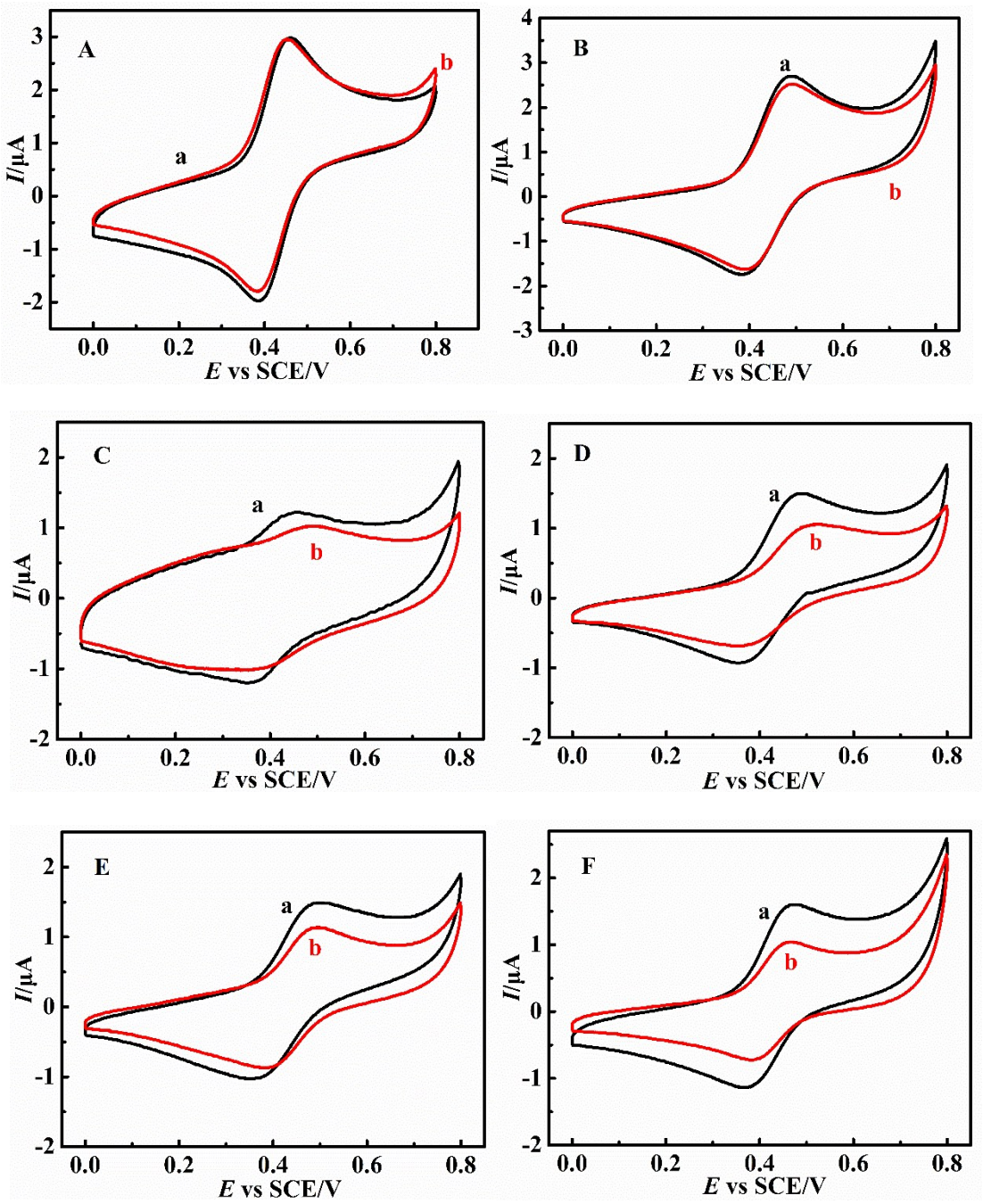

Fig. S8 CVs of 0.5 mM FDA at 0.1 V s^{-1} at (A) bare Au, (B) PDMA film, (C) PNIPA film, (D) P(DMA-*co*-NIPA) film, (E) P(DMA-*co*-NIPA)/AuNCs film and (F) P(DMA-*co*-NIPA)/TPE film electrodes in pH 5.0 buffers containing (a) 0 and (b) 0.6 M Na_2SO_4, respectively.

3.4 Switchable electrocatalytic oxidation of NADH mediated by FDA at P(DMA-*co*-NIPA)/AuNCs/TPE film electrodes

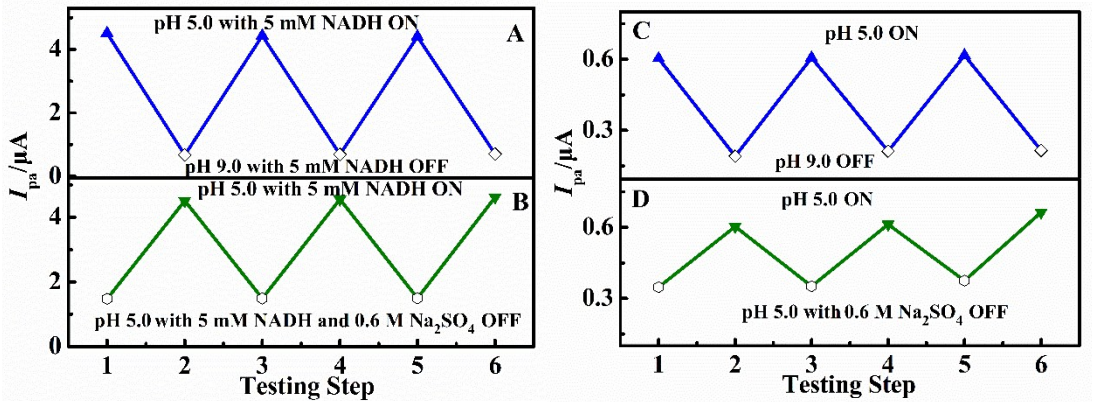

Fig. S9 Variation of CV I_{pa} of 0.5 mM FDA at 0.01 V s^{-1} for P(DMA-*co*-NIPA)/AuNCs/TPE films with (A) the solution pH switched between 5.0 and 9.0 with 5 mM NADH, (B) the Na_2SO_4 concentration cycled between 0 and 0.6 M at pH 5.0 with 5 mM NADH, (C) the solution pH switched between 5.0 and 9.0 and (D) the Na_2SO_4 concentration cycled between 0 and 0.6 M at pH 5.0, respectively.

3.5 Synergetic effect of pH and Na_2SO_4 on fluorescence responses of P(DMA-*co*-NIPA)/AuNCs/TPE films

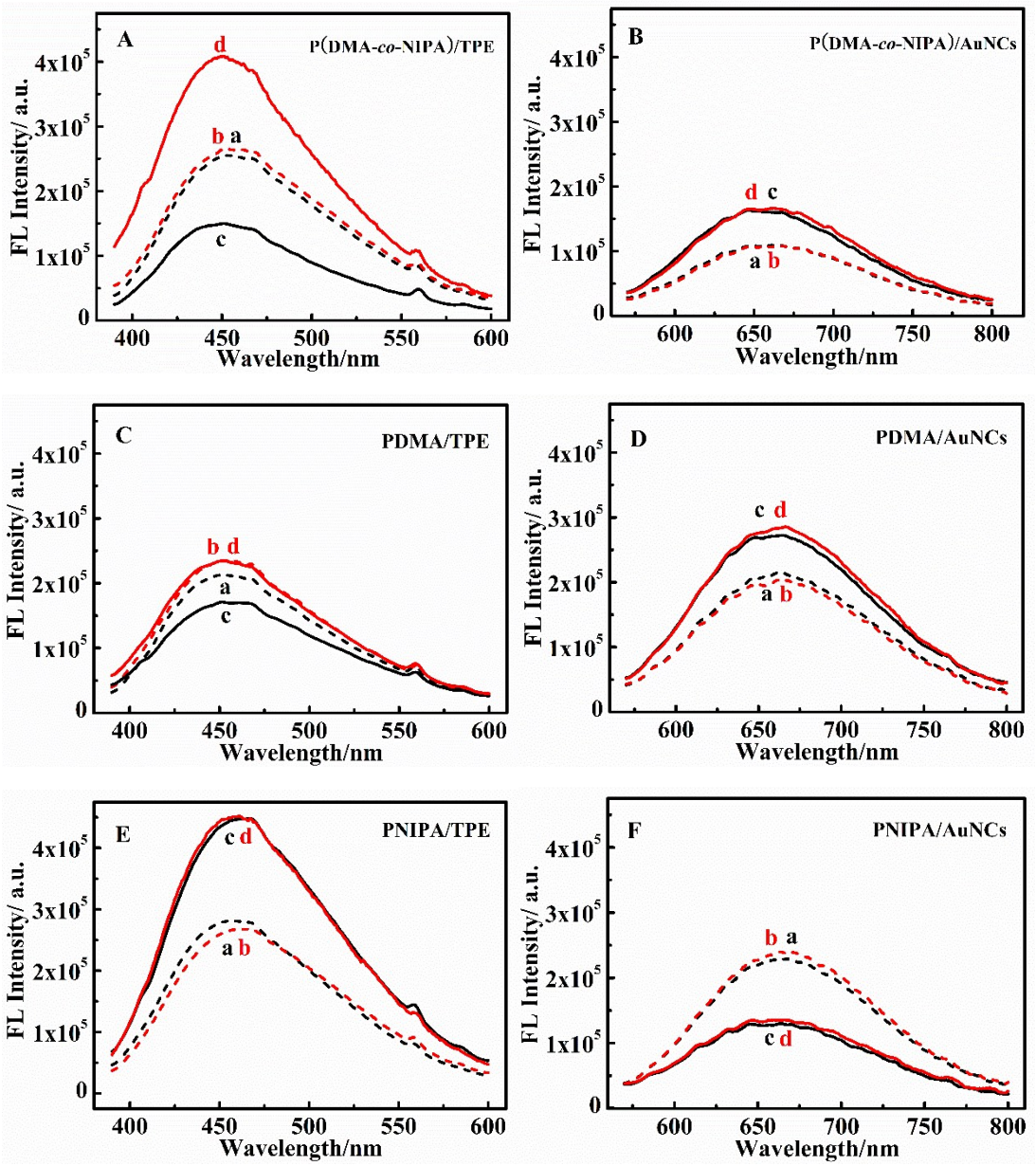

Fig. S10 FL spectra of (A) P(DMA-*co*-NIPA)/TPE, (B) P(DMA-*co*-NIPA)/AuNCs, (C) PDMA/TPE, (D) PDMA/AuNCs, (E) PNIPA/TPE and (F) PNIPA/AuNCs films in (a) pH 5.0 buffers, (b) pH 9.0 buffers, (c) pH 5.0 buffers with 0.6 M Na_2SO_4 and (d) pH 9.0 buffers with 0.6 M Na_2SO_4. The scales of Y-axis in all the figures were kept the same so that the peak intensities in different figures could be easily comparable.

3.6 Construction of 4-input/9-output logic gates

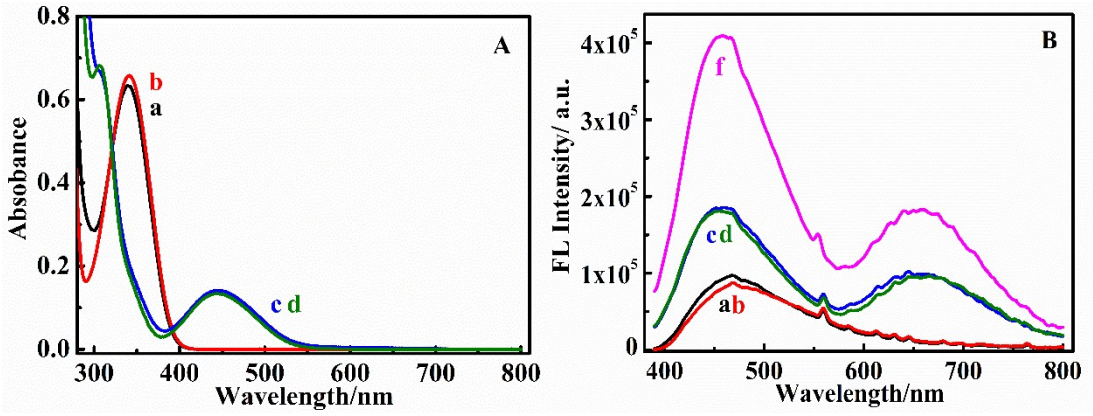

Fig. S11 (A) UV-vis absorption spectra of 0.1 mM NADH in (a) pH 5.0 and (b) pH 9.0 buffers, and 0.5 mM FDA in (c) pH 5.0 and (d) pH 9.0 buffers. (B) FL spectra with the excitation at 330 nm of P(DMA-*co*-NIPA)/AuNCs/TPE films in 5 mM NADH solutions at (a) pH 5.0 and (b) pH 9.0, and in 0.5 mM FDA solutions at (c) pH 5.0 and (d) pH 9.0, and (f) pH 9.0 with 0.6 M Na_2SO_4, respectively.

3.7 Establishment of encoder, decoder and demultiplexer

An encoder is a non-Boolean device and is used for compressing data.[1,2] For example, 2 input bits can be condensed into 1 output bit by a 2-to-1 encoder. With P(DMA-*co*-NIPA)/AuNCs/TPE film electrode in the solution containing 0.5 mM FDA and 5 mM NADH as the working platform, a 2-to-1 encoder could be established, where pH (Input A) and Na_2SO_4 (Input B) were chosen as the two inputs, and the CV I_{pa} at 0.5 V (Output I_3) as the single output. The definitions of these inputs and output were the same as in Table 1. For the input combination (01), Output I_3 was at the 0 state because the bioelectrocatalysis of NADH mediated by FDA could still be clearly observed in pH 5.0 buffers with Na_2SO_4, making the CV I_{pa} at 0.5 V larger than the

threshold of 1 μA (Fig. 4B, curve c). However, for the input combination of (10), Output I_3 was at the 1 state since the electrocatalysis of NADH mediated by FDA was suppressed greatly in pH 9.0 buffers even without Na_2SO_4, resulting in the CV I_{pa} at 0.5 V smaller than the threshold of 1 μA (Fig. 4B, curve b). The truth table and schematic diagram of the encoder are presented in Fig. S12A.

A

Input A (pH)	Input B (Na_2SO_4)	Output I_3 (I_{pa} at 0.5 V)
0	1	0
1	0	1

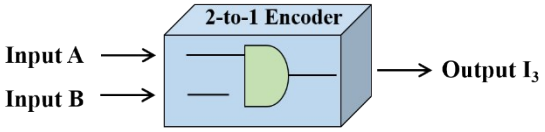

B

Input B (Na_2SO_4)	Output F_2 (FL_{450})	Output F_4 (FL_{660})
0	1	0
1	0	1

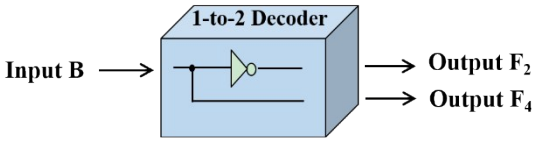

Fig. S12 Truth table and symbolic representation of (A) a 2-to-1 encoder with pH and Na_2SO_4 as 2 inputs and CV I_{pa} at 0.5 V as the output and (B) a 1-to-2 decoder with Na_2SO_4 as the input and F_2 (FL_{450}) and F_4 (FL_{660}) as 2 outputs.

In contrast with an encoder, a decoder, also a non-Boolean device, transforms fewer inputs into more outputs [1, 2]. For instance, a 1-to-2 decoder can turn 1 input datum to 2 output codes. With P(DMA-*co*-NIPA)/AuNCs/TPE film electrodes in pH 9.0 buffers without FDA and NADH as the working platform, a 1-to-2 decoder could be developed. Herein, Na_2SO_4 (Input B) was adopted as the sole input, and FL_{450} (Output F_2) and FL_{660} (Output F_4) were selected as the two outputs. The definitions of these input and outputs were the same as in Table 1. When Input B was at the 0 state, Output F_2 was at the 1 state because the FL_{450} of the films could be kept at the modest level in

the absence of Na_2SO_4 in pH 9.0 solutions. Concurrently, Output F_4 was at the 0 state since FL_{660} of the system was smaller than the threshold of 1.3×10^5 without the enhancement from Na_2SO_4. When input B was at the 1 state, Output F_2 was at the 0 state since the addition of Na_2SO_4 in pH 9.0 buffers would lead to the highest level of FL_{450}, larger than the threshold of 3.5×10^5. In the meantime, Output F_4 was at the 1 state because the FL_{660} of the films would be increased in the presence of Na_2SO_4 in pH 9.0 solutions, and larger than the threshold of 1.3×10^5. The truth table and symbolic diagram of the 1-to-2 decoder are manifested in Fig. S12B.

3.8 Fabrication of various keypad locks

For the 2-input/1-output keypad lock, designated as Keypad Lock1, P(DMA-*co*-NIPA)/AuNCs/TPE film electrodes in pH 5.0 buffers served as the initial state. The two operations were defined as 2 inputs: the irradiation of UV excitation light at 330 nm as Input U and the addition of 5 mM NADH in solution as Input N. The FL intensity at 660 nm (FL_{660}) collected immediately after Input U was selected as Output FL_1 with 6.5×10^4 as the threshold. Only when Output FL_1 was at the 1 state, the keypad lock could be unlocked. The detailed descriptions of the inputs and outputs, and the corresponding thresholds are presented in Fig. S13A. The truth table and the corresponding histogram with all the 2 possible sequences of the 2 inputs are presented in Fig. S13B and C, respectively.

A

Input	
U	N
UV excitation light at 330 nm	5 mM NADH

Output	
	FL_1 (FL_{660})
1	$> 6.5 \times 10^4$
0	$\leq 6.5 \times 10^4$

B

Input sequence		Output FL_1
U	N	1
N	U	0

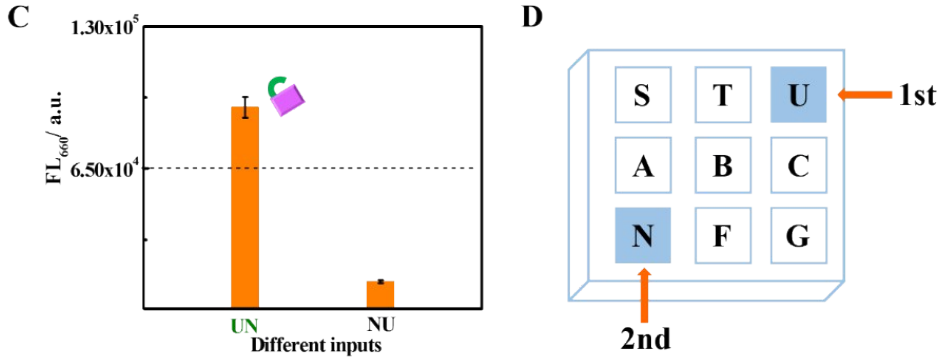

Fig. S13 (A) Definitions of 2 inputs and 1 output and (B) truth table of Keypad Lock1. (C) Histogram of the FL intensity at 660 nm (FL_{660}) for the two sequences of the two inputs. The threshold is indicated via the dashed line. Error bars mean the standard deviation of 3 repetitive experiments. (D) The corresponding schematic diagram of the keypad lock system with 2 correct inputs.

For the UN sequence, the irradiation of UV light at the first step led to the FL_{660} higher than the threshold of 6.5×10^4, Output FL_1 was thus at the 1 state, because the absence of NADH in solution would result in no quenching effect. After the first step, the addition of NADH at the second step would no longer affect the Output FL_1 since the FL_{660} had already been measured. However, for NU sequence, because of the addition of NADH in the first step, the irradiation of UV light at the second step would lead to the extremely small FL_{660} due to the quenching effect of NADH, Output FL_1

was at the 0 state. Thus, only the input order of UN could open the keypad lock.

A

Input		
C	U	F
CV test	UV excitation light at 330 nm	0.5 mM FDA

Output		
	IP_2 I_{pa} at 0.5 V (μA)	FL_3 FL_{450}
1	> 0.4	> 2.0×10^5
0	≤ 0.4	≤ 2.0×10^5

B

Input sequence			Output IP_2	Output FL_3
C	U	F	0	1
C	F	U	0	0
U	C	F	0	1
U	F	C	1	1
F	C	U	1	0
F	U	C	1	0

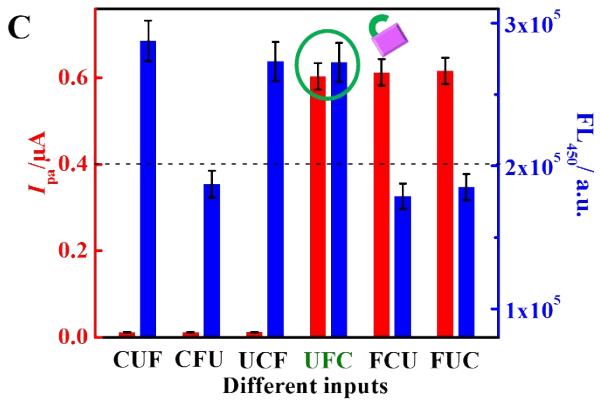

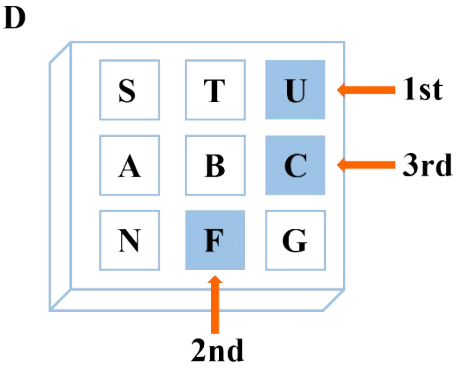

Fig. S14 (A) Definitions of 3 inputs and 2 outputs and (B) truth table of Keypad Lock3. (C) Histogram of CV I_{pa} at 0.5 V (left) and the FL intensity at 450 nm (right) for different sequences of the 3 inputs. The threshold is indicated via the dashed line. Error bars mean the standard deviation of three repetitive experiments. (D) The corresponding schematic diagram of the keypad lock system with 3 correct inputs.

REFERENCES

1 J. Andreasson, S. D. Straight, T. A. Moore, A. L. Moore and D. Gust, *J. Am. Chem. Soc.*, 2008, **130**, 11122.

2 S. Liu, M. Li, X. Yu, C.-Z. Li and H. Liu, *Chem. Commun.*, 2015, **51**, 13185.